SURFACE AND INTERFACE MODIFICATION OF ALTERNATIVE SEMICONDUCTOR MATERIALS FOR ADVANCED TRANSISTORS

By

QI JIANG

A Thesis submitted to the

Graduate School-New Brunswick

Rutgers, The State University of New Jersey

in partial fulfillment of the requirements

for the degree of

Master of Science

Graduate Program in Chemistry and Chemical Biology

written under the direction of

Professor Eric Garfunkel

and approved by

_____

_____

_____

New Brunswick, New Jersey

October, 2009

ABSTRACT OF THESIS

Surface and Interface Modification of Alternative Semiconductor Materials for Advanced Transistors

By QI JIANG

Thesis Director:
Professor Eric Garfunkel

Alternative semiconductor materials have the potential to replace silicon in next generation transistors. However, the lack of a stable insulating oxide such as SiO_2 with high quality electrical properties prevents the further fabrication of competitive metal oxide semiconductor field effect transistors (MOSFETs). Germanium and gallium arsenide, two widely investigated semiconductor materials, have high prospects for generating high quality surfaces and interfaces between the dielectric layer and the semiconductor.

In this thesis, wet chemistry cleaning methods have successfully removed the native oxide and other impurities on the Ge and GaAs surface. With further sulfur passivation in $(NH_4)_2S$ solution, a clean passivated Ge and GaAs surface can be formed which shows appropriate stability and reliability

for fabrication. Physical and chemical characterization has been performed on multilayer film structures after the high-κ dielectric films are grown by atomic layer deposition. Electric properties of the MOSFET confirm that the sulfur passivation has greatly decreased the interface state density. The convenience and low cost of wet chemistry cleaning and passivation provide a reliable strategy for the application of alternative semiconductor materials like Ge and GaAs in future transistors and related devices.

Acknowledgements

I would like to gratefully acknowledge the enthusiastic supervision of Professor Eric Garfunkel during my work in Rutgers University. I am very grateful to thank Dr. Chien-Lan Hsueh for his great help, instruction, and discussion of my research work. I thank Dr. Lei Yu, Dr. Alan S. Wan, Ozgur Celik, Lauren Klein, Daniel Mastrogiovanni and Yi Xu in the research group. They helped me a lot during my work in the lab and the writing of this thesis. Tian Feng and Dr. Hang-Dong Lee helped me for the MEIS analysis and thank you so much.

I wish to express my gratitude to all the friends in Rutgers University. It is a good memory to work with all of you for the past three years.

I also address my special thanks to my girlfriend and my parents during this period. They give me the great support and help to continue the studies in my life.

Qi Jiang

May 2009

List of Abbreviation

ALD	Atomic Layer Deposition
ALE	Atomic Layer Epitaxy
CVD	Chemical Vapor Deposition
DIW	De-Ionized Water
MEIS	Medium Energy Ion Scattering
MOSFET	Metal Oxide Semiconductor Field Effect Transistor
PVD	Physical Vapor Deposition
RBS	Rutherford Backscattering Spectroscopy
TEM	Transmission Electron Microscope
TMA	Trimethylaluminium
TEMAHf	Tetrakis(ethylmethylamide)hafnium
UHV	Ultra High Vacuum
XPS	X-ray Photoelectron Spectroscopy

Table of Contents

Title Page·····i

Abstract·····ii

Acknowledgement·····iv

List of Abbrevation·····v

Table of Contents·····vi

List of Tables and Illustrations·····viii

Chapter 1 Introduction·····1

1. Alternative semiconductor materials and surface passivation·····1

2. The growth of High-κ dielectric film by Atomic Layer Deposition (ALD)·····4

3. Structure of the Thesis·····8

Chapter 2 Experimental methods and characterizations·····9

1. Wet chemistry surface cleaning for substrates·····9

2. Sulfur passivation·····9

3. ALD experiments·····10

4. Surface and interface analysis·····10

Chapter 3 Results and Discussions·····12

1. Wet chemistry cleaning and sulfur passivation of Ge·····12

2. Wet chemistry cleaning and sulfur passivation of GaAs·····19

3. Atomic Layer Deposition of High-κ dielectric films on Ge and GaAs··23

Chapter 4 Conclusion·····27

Reference·····29

List of Tables and Illustrations

Table 1 Properties of different semiconductor materials at 300K····· 1

Figure 1 Dangling bond on the Ge(111) surface (side view) ····· 2

Figure 2 Scheme of MOSFET device with a high-κ dielectric and a high mobility semiconductor channel····· 4

Figure 3 Schematic drawing of one ALD cycle of HfO_2 film with the $Hf(NCH_3C_2H_5)_4$ (TEMAHf) precursor and H_2O····· 6

Figure 4 The integrated ALD, XPS, and metallization system····· 7

Figure 5 Ge 3d XPS spectra from as-received Ge(100)····· 12

Figure 6 Ge 3d XPS spectra from HF/DIW cyclic treated Ge(100)····· 13

Figure 7 Ge 3d XPS spectra from H_2O_2 treated Ge(100)····· 14

Figure 8 Ge 3d XPS spectra from H_2SO_4/H_2O_2 treated Ge(100) ····· 14

Figure 9 Ge 3d XPS spectra of sulfur passivated Ge(100) after cleaning····· 16

Figure 10 C 1s XPS spectra from sulfur passivated Ge(100) sample with different wet chemistry treatments····· 17

Figure 11 MEIS spectra of a sulfur passivated Ge(111) surface with interface depth profiling and element density analysis····· 18

Figure 12 Ga and As 3d XPS spectra of as-received GaAs(100) ····· 20

Figure 13 Ga and As 3d XPS spectra of sulfur passivated GaAs(100) after HCl and NH_4OH cleaning····· 21

Figure 14 As 2p XPS spectra of as-received (upper) and sulfur passivated (lower) GaAs(100)····· 22

Figure 15 RBS spectra and growth rate of ALD with HfO_2/Ge····· 24

Figure 16 RBS spectra and growth rate of ALD with HfO_2/GaAs····· 25

Figure 17 Cross sectional TEM image of the MOS gate stack TaN/HfO_2/GaAs····· 26

Chapter 1 Introduction

1. Alternative Semiconductor Materials and Surface Passivation

With the rapid development of modern microelectronics, higher packing density and lower power dissipation metal-oxide-semiconductor field-effect transistor (MOSFET) devices have been improved primarily by physical scaling [1]. There is a strong motivation to continue scaling MOSFETs with higher channel mobility using various alternative materials in place of silicon. Germanium and gallium arsenide [2], in particular, are actively investigated, and MOSFET have already been demonstrated. In Table 1 the material characteristics of these potential channel materials are listed [3].

Properties	Si	Ge	GaAs
Atomic Weight	28.09	72.60	144.64
Crystal Structure	Diamond	Diamond	Zincblende
Density (g/cm^3)	2.329	5.327	5.317
Lattice Constant (Å)	5.43102	5.64613	5.6533
Electron Affinity (V)	4.05	4.0	4.07
Energy Band Gap (eV)	1.12	0.66	1.42
Electron Mobility ($cm^2/V\text{-}s$)	1450	3900	8000
Hole Mobility ($cm^2/V\text{-}s$)	500	1900	400

Table 1 Properties of different semiconductor materials at 300K.

For more than 40 years, the primary semiconductor material for transistors and integrated circuits has been Si. The choice of Si over other semiconductors is often attributed to its oxide (SiO_2), which serves to passivate the Si and form a defect-free interface between the Si and SiO_2. The oxide has traditionally been used for the dielectric in MOSFET transistors. The superb interface that forms naturally between Si and SiO_2 is critical to the operation of the transistor, as the interface between the dielectric and semiconductor greatly influences the electrical properties of the device [4].

Ge and GaAs offer great potential for replacing Si to achieve high mobility. In fact, it has long been known that Ge and GaAs have better inherent electrical properties than Si. The very first transistor in 1947 was made of Ge and Ge-based MOSFETs have been studied for decades [5]. Moreover, heterostructures of III-V semiconductors have been widely used in the optoelectronic devices [6]. Even though the mobility-related advantages are apparent, Ge and GaAs have not been developed in MOSFET primarily because the surface is not effectively passivated with native oxides. The lack of a good passivation oxide results in a high leakage current rate and high density of interface state [7]. For the further application of high mobility channel semiconductor materials, surface modification and passivation are necessary before device fabrication.

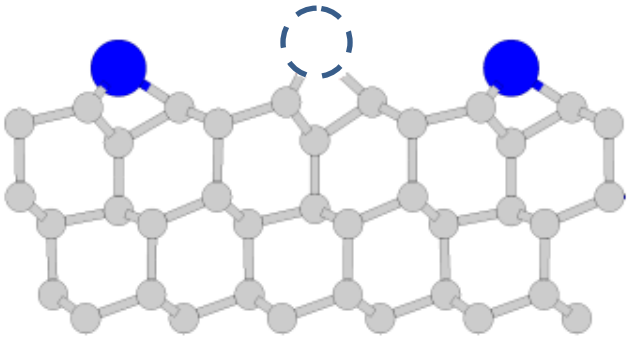

Figure 1 Dangling bond on the Ge(111) surface (side view).

One of the main issues that arise in considering new semiconductors such as Ge and GaAs is the need for surface preparation and passivation strategies. Figure 1 indicates the defects and dangling bonds on the Ge surface [8]. An effective passivation treatment should be chemically stable, protect the substrate from unwanted oxidation and contamination, as well as help minimize interface or surface-induced carrier recombination [9]. Although an ideally passivated surface would resist oxidation and degradation perfectly, such complete resistance is not possible in practice. We consider passivated surfaces that strengthen resistance to oxidation in both ambient air and aqueous solution [4]. Three different surface passivation layers are investigated: sulfur [10-14], chloride [15, 16] and hydride [17, 18]. Actually, sulfur passivation creates the most ideal results, whereas both chloride and hydride add limited stability, which is sufficient to alter the surface reactivity. Sulfur passivation can also be accomplished with wet chemical functionalization; it is more desirable in industry because of its simplicity and low cost [18].

The surface cleaning of alternative semiconductors is very crucial in the fabrication of MOSFET devices. Unlike Si, both Ge and GaAs have different compositions and stabilities of native oxides on the surface, which will affect the quality and electrical properties of the resulting devices. The common cleaning procedures for semiconductor substrates usually involve three steps: (1) degreasing, (2) chemical etching to remove native oxide and other impurities, and (3) growth of a protective oxide layer (which is often removed, for example by annealing, in a controlled environment right before the further fabrication) to ensure a clean substrate. However, steps 2 and 3 are quite challenging for the cleaning of Ge and GaAs to produce a surface appropriate to the production of

MOSFET devices, and it requires different chemical reagents and treatments for the semiconductor materials with wet chemistry methods.

2. The growth of high-κ Dielectric film by Atomic Layer Deposition (ALD)

Thermally grown SiO_2 has been used as a gate dielectric since the introduction of MOSFET devices. Because SiO_2 has high compatibility with the Si substrate, a relatively simple growth process on Si, and excellent insulator properties, Si has been the leading semiconductor for decades. With the further development and scaling of devices, as the SiO_2 gate oxide is scale below 1.5 nm, it permits a dramatic increase in the direct tunnel leakage current through the insulator and reduces the drive current, which leads to a high power loss and break-down of the device [19].

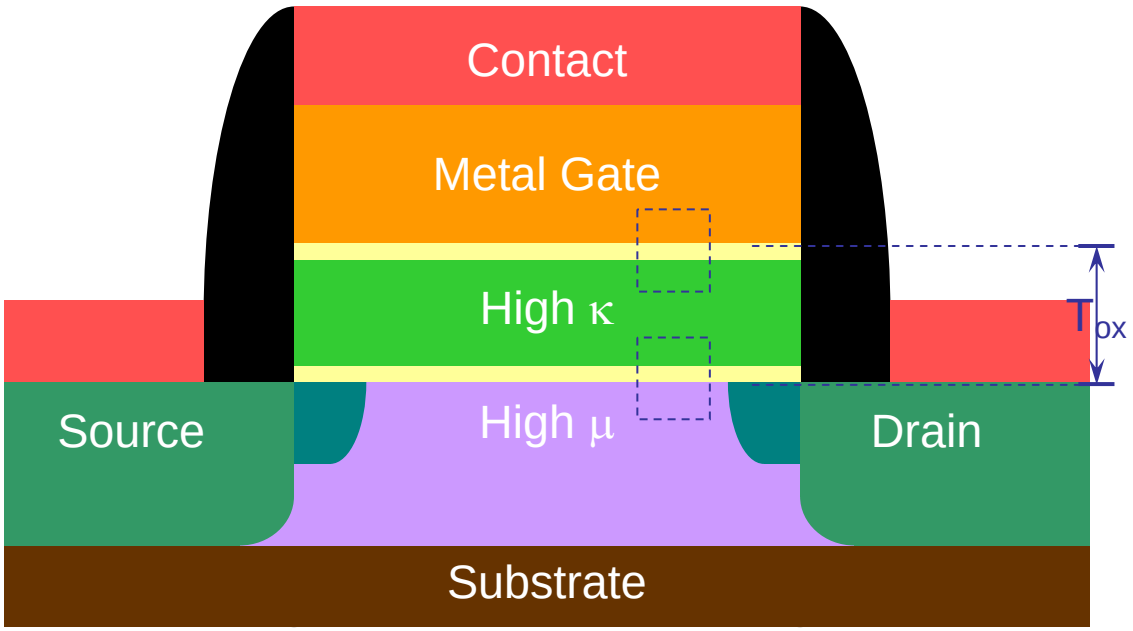

Figure 2 Scheme of MOSFET device with a high-κ dielectric and a high mobility (high-μ) semiconductor channel

The high leakage current and the inadequate reliability of the SiO_2 layer when it is less than 1 nm suggests a need for a replacement of SiO_2 with a thicker dielectric material with higher permittivity (κ). High-κ dielectrics reduce the leakage current by providing a thicker film while electrically behaving as a thinner equivalent dielectric [20]. Therefore high-κ materials are excellent candidates for replacements to the traditional SiO_2 gate oxide. Figure 2 shows us the scheme of a MOSFET structure with a high-κ dielectric film and an alternative semiconductor (high-μ).

From a process point of view, candidates for alternative gate dielectrics must meet a set of criteria such as thermodynamic stability, interface quality, and film morphology [20]. Many dielectric materials have been investigated, but very few appear promising with respect to all the guidelines listed above. Furthermore, an alternative gate dielectric should have low oxygen diffusivity, a low density of defects and a high thermal stability with the substrate, so that interfacial reactions with the adjacent layers are minimized. The requirements mentioned above limit the gate dielectric candidates to only a few, among which the oxides, such as Al_2O_3 [21-24], HfO_2 [25-28], ZrO_2 [29-31] and Ta_2O_5 [32-34] are the most promising. Oxides of binary alloys, such as $ZrAl_xO_y$ [35, 36] have also been studied because of the attempt to combine the desirable qualities of the special properties in industrial materials.

Atomic layer deposition (ALD), originally known as Atomic layer epitaxy (ALE), was invented by Finnish scientists Suntola and Antson in the middle of 1970s for the fabrication of thin film electroluminescence displays where high quality insulating and luminescent films on large area substrates were required [37, 38]. However, with the down-scaling of semiconductor device dimensions, the requirements of thin-film

technology have grown enormously and ALD has found new opportunities in MOSFET devices and high density memory devices with strong level integration. Some leading alternative high-κ dielectrics such as Al_2O_3, HfO_2 and ZrO_2 are deposited by ALD with different types of precursors [39].

Different from chemical vapor deposition (CVD) and physical vapor deposition (PVD), ALD is based on sequential and saturating surface reactions of alternately applied precursors [40]. ALD consists of four essential steps: 1) precursor exposure, 2) evacuation or purging of the precursors and any byproducts from the chamber, 3) exposure of the reactant species, typically oxidants or other reagents, and 4) evacuation or purging of the reactants and byproduct molecules from the chamber. Figure 3 illustrates the scheme of

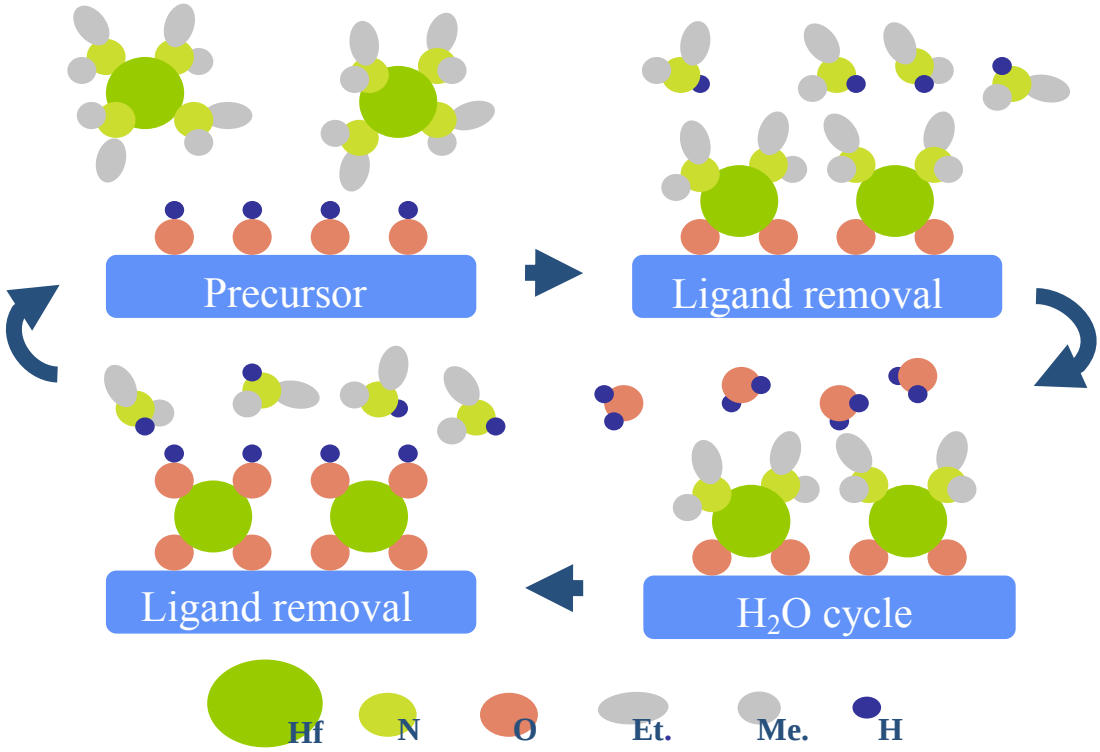

Figure 3 Schematic drawing of one ALD cycle of HfO_2 film with the $Hf(NCH_3C_2H_5)_4$ (TEMAHf) precursor of and H_2O

one ALD cycle for HfO_2 film growth with the organometallic precursor and water. Although there are many similarities between ALD and CVD, the clear and distinctive feature of ALD lies in the self-limitation for precursors and reactants. The excellent conformality, atomic scale thickness control, and low growth temperature determine the great importance of ALD for novel device fabrication.

In our work, ALD of high-κ dielectrics were performed in a homemade ALD system coupled to a commercial x-ray photoelectron spectroscopy (XPS) system shown schematically in Figure 4. The ALD system consists of a sample introduction chamber, a reactor with a sample heater, and gas lines. The sample holder which is compatible with the XPS system is loaded into the reactor from the quick load lock. The gate vale between the reactor and the load lock makes it possible to load a sample without venting the reactor. Together with the metallization chambers which have the ability to deposit various metals

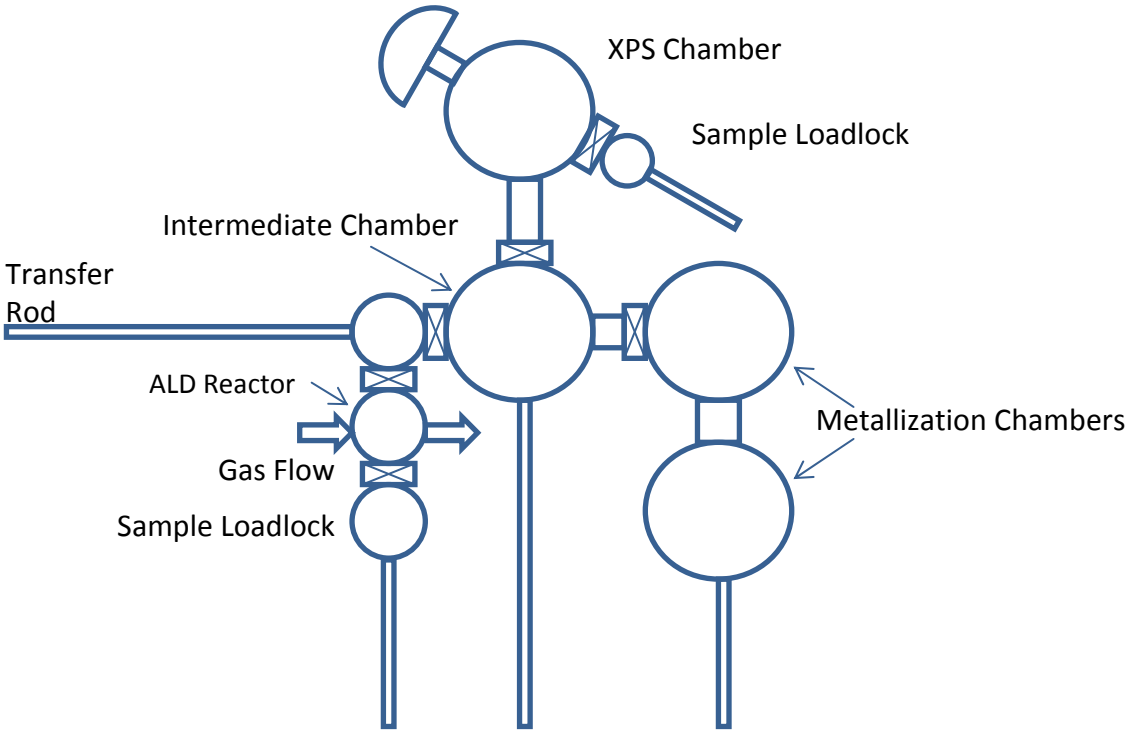

Figure 4 The integrated ALD, XPS, and metallization system

with evaporation and sputtering as the metal gate, and this integrated system makes *in-situ* study of advanced MOSFET devices possible. With direct ALD reaction for thin film growth and XPS analysis, the details of surface characterization can be investigated *in-situ*, and different conditions can be controlled and optimized.

3. Structure of the Thesis

Chapter 1 outlines the research background and the potential significance of alternative semiconductors in transistors, ALD for high-κ dielectrics, as well as instrumental characterization.

Chapter 2 describes the experiment process with chemistry, as well as a more detailed description of instrumental characterization.

Chapter 3 reviews the results of the experiment of wet chemistry cleaning, sulfur passivation and surface analysis. With further analysis, it provides the basis of a more in depth discussion and reveals the significance of the work.

Chapter 4 concludes the thesis and proposes future work.

Chapter 2 Experiments and Characterizations

1. Wet Chemistry Surface Cleaning of Substrates

All the semiconductor substrates were degreased in organic solvents with 1) methanol and 2) acetone in the ultrasonic bath for 10 min each. After total rinsing with de-ionized water (DIW) and drying with nitrogen gas, the Ge substrate was cleaned with concentrated sulfuric acid (H_2SO_4) and 30% hydrogen peroxide (H_2O_2) with the volume ratio at 4:1 for 10 min. GaAs substrate was cleaned with 9% hydrochloric acid (HCl) for 3 min and 5% ammonium hydroxide (NH_4OH) for 10 min. After cleaning, the substrate was cleaned with methanol or placed in pure methanol until use. Other chemical reagents including hydrofluoric acid (HF) were also explored, but did not result in MOS capacitors with high electrical quality interfaces.-

2. Sulfur Passivation

We use commercial aqueous 48% ammonium sulfide $(NH_4)_2S$ solution for the sulfur passivation of all the substrates at 70-80°C for 15 min. The substrates were rinsed with methanol and soaked in pure methanol after the passivation. We also tried saturated solutions of thioacetamide and thiourea for the sulfur passivation; however our results were not promising with these chemistries.

All the glassware and tweezers for the wet chemistry and sulfur passivation were cleaned by standard "RCA clean" methods. Sulfur passivation glassware and tweezers were again cleaned immediately after the experiments.

3. ALD Experiments

In order to grow high-κ dielectric films, we chose trimethylaluminum $Al(CH_3)_3$ (TMA) and Tetrakis(ethylmethylamide)hafnium $Hf(NCH_3C_2H_5)_4$ (TEMAHf) as precursors for the ALD deposition of Al_2O_3 and HfO_2. The oxygen source was H_2O. The corresponding growth temperatures for Al_2O_3 and HfO_2 were 95°C and 170°C. The reaction cycle was adjusted by different conditions with different pressures for the experiments. The whole ALD system was monitored and controlled with a LabView program running on a PC. With a Baraton pressure gauge and thermocouples attached to the sample, the reactor, gas lines and precursor bottles, the pressure and temperatures were logged at all times. Using the LabView program, we can easily configure temperature set points for each part of the system and design customized ALD growth parameters including gas pulse sequence, duration, and number of cycles.

4. Surface and Interface Analysis

We mainly used XPS for the analysis of surface elemental composition and chemical state of all the samples. After the ALD growth, the different film growth thickness and area density were also quantified by Rutherford backscattering spectroscopy (RBS). For

analysis of surface composition and depth profiling of the sample, the medium energy ion scattering (MEIS, a high depth resolution variant of RBS) was also used for surface and interface composition. We also did some cross sectional analysis using transmission electron microscope (TEM) to determine the composition and interface structure of the MOS gate stack.

Chapter 3 Results and Discussions

1. Wet Chemistry Cleaning and Sulfur Passivation of Ge

On a Ge substrate, the formation of a non-permeable protective oxide layer has been considered impractical because GeO_2 has a high water-solubility and can even be dissolved by moisture from air. Figure 5 indicates the XPS Ge 3d spectra of an as-received Ge (100) sample and the number in parenthesis for each peak denotes the corresponding chemical shift in eV. The major peak at 29 eV is related to the elemental Ge originating from the substrate [41], and the other peak at 32.5 eV is in good agreement with GeO_2 [42]. In order to obtain the best fit, we also need to include two small peaks at 31.2 eV and 30.5 eV, and both of them are determined as GeO and GeC correspondingly [42, 43]. The XPS results show us that the native oxide consists mostly of GeO_2 and a small amount of GeO as well as some impurity carbide species.

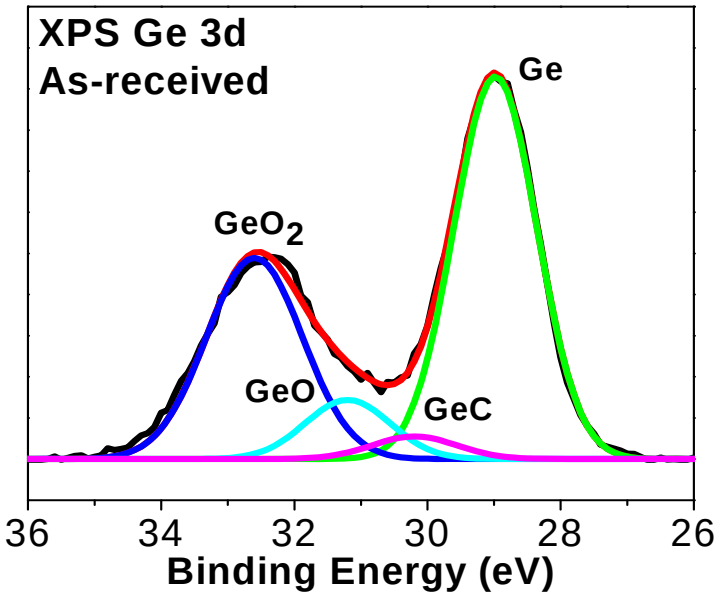

Figure 5 Ge 3d XPS spectra from as-received Ge(100)

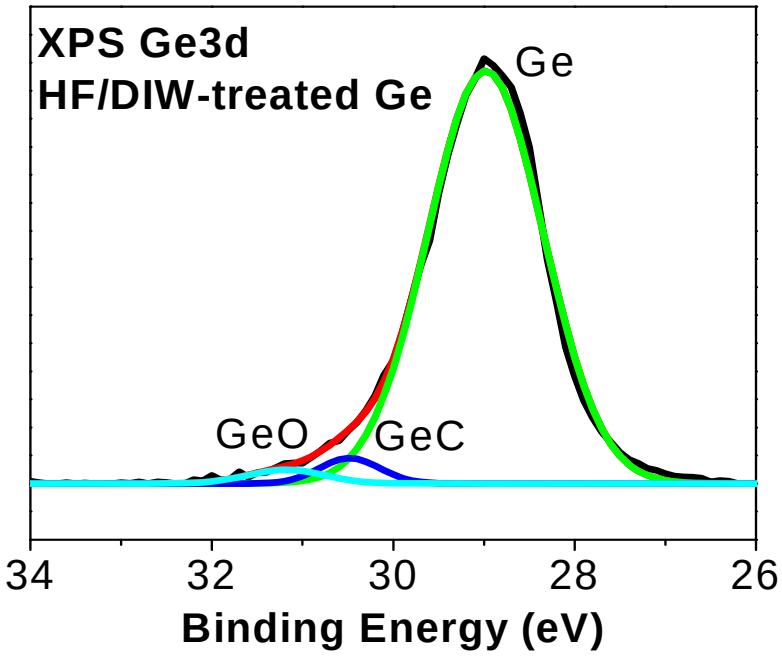

Figure 6 Ge 3d XPS spectra from HF/DIW cyclic treated Ge(100)

HF is often used to etch the native oxide layer and produce a hydrogen terminated surface Si. The use of concentrated HF solution (49%) on Ge should be avoided because such concentrated HF increases the roughness of the surface; the roughening is presumed to be due to the Ge back-bond breaking during HF etching [16]. It has been determined that cyclic HF/DIW rinsing is effective in removing the native oxide [44]. For the treatment of cyclic HF/DIW rinses, Ge samples are rinsed in DIW, dipped in diluted HF solution (10%) and rinsed in DIW again. This procedure is repeated for 3 to 5 times in order to peel off the oxide layer. Figure 6 indicates the Ge 3d XPS spectra from a Ge(100) sample after cyclic rinsing of HF/DIW. From the figure, we can find that the GeO_2 is completely removed, but the peaks of GeO and GeC are still present. In fact, it has been shown that HF treatment always leaves behind sub-oxides and carbides [16].

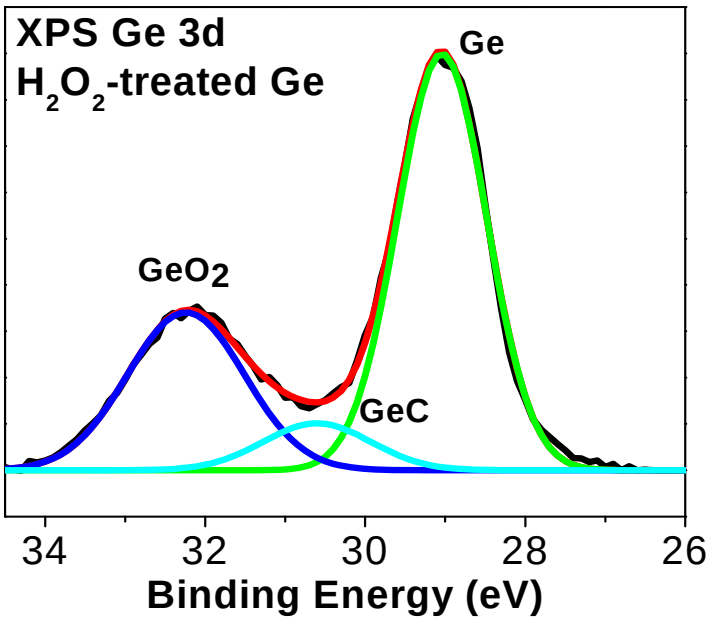

Figure 7 Ge 3d XPS spectra from H_2O_2 treated Ge(100)

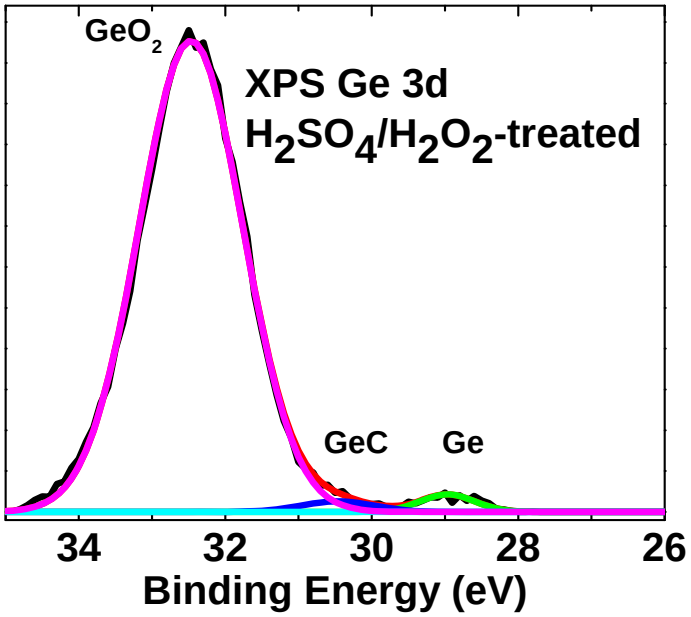

Figure 8 Ge 3d XPS spectra from H_2SO_4/H_2O_2 treated Ge(100)

Since it is difficult to completely remove oxide and carbon from Ge substrates, different approaches were explored involving the transformation of these into other chemical

species which are easier to remove. On the Ge sample, we propose to oxidize the sub-oxide and carbide with some chemical oxidants and generate a protective chemical oxide layer [45, 46]. H_2O_2 is often used in wet chemical oxidation, because it has a high reaction efficiency and does not result in the incorporation of other elements. In this work on Ge, we have compared chemical oxides formed by concentrated H_2O_2 and a mixture of H_2SO_4/H_2O_2 (v/v=4/1). The reasons for using H_2SO_4 with H_2O_2 for oxidation are: (1) H_2SO_4 helps remove hydrocarbons, and (2) the oxidation of H_2O_2 in the acid reaction is stronger and more effective in converting GeO and GeC. The Ge 3d XPS spectra with chemical oxides formed by these two solutions are shown in Figures 7 and 8. With both results, the GeO signals are not detectable and the intensities of the GeC peaks are small. After the H_2SO_4/H_2O_2 treatment, a clean Ge surface without oxide and carbide can be easily obtained using water to dissolve the GeO_2. However, we find that hydrocarbon and other contamination easily returns to the clean Ge surface if this protective oxide layer is removed.

After the preparation of a clean Ge surface, we employ an appropriate chemistry to obtain sulfur passivation on the Ge surface. It has been demonstrated that 1 monolayer of elemental sulfur can be deposited on Ge (100) to form an ideal 1×1 S-terminated surface in ultra-high vacuum (UHV) [10, 11]. However, the high cost and inconvenience of UHV methods would be virtually impossible to realize by the semiconductor industry at a reasonable cost. To prepare a sulfur passivated Ge surface with wet chemistry, 48% $(NH_4)_2S$ solution is used [14, 47]. After being heated to 70-80°C for 15 min, the Ge sample is rinsed with methanol to remove excess $(NH_4)_2S$ and dried by N_2. In our study, Ge samples which are later used for ALD growth are first pretreated with H_2SO_4/H_2O_2 to

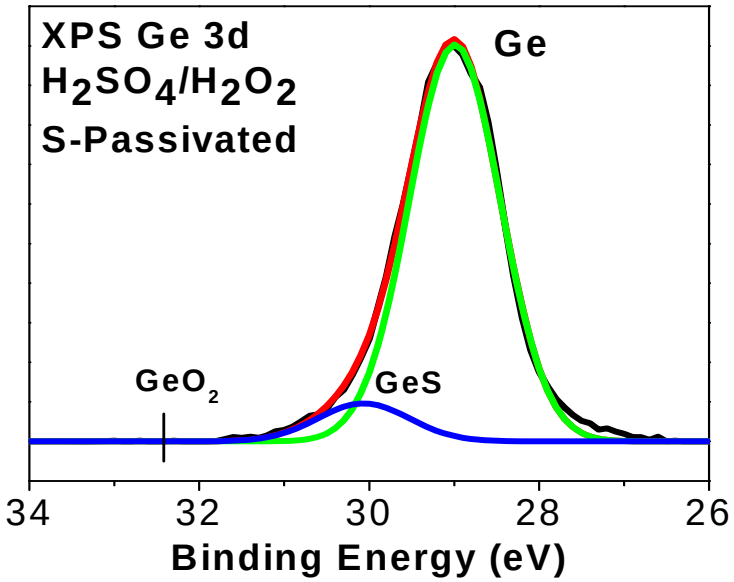

Figure 9 Ge 3d XPS spectra of sulfur passivated Ge(100) after cleaning

remove the native oxide and grow a protective chemical oxide layer on the surface. Figure 9 shows Ge 3d XPS spectra of a Ge sample which has undergone such a treatment. In the figure, the peak with a 3 eV chemical shift corresponding to GeO_2 disappears which implies that the chemical oxide is completely removed by a hot aqueous $(NH_4)_2S$ solution. Moreover, a broad shoulder peak after fitting is present due to the surface Ge atoms bonded to S atoms. In previous studies, this has been attributed to one layer of bridge-bonded S atoms on the Ge surface [10, 11]. Saturated solutions of thioacetamide and thiourea also have been reported as effective passivation reagents [48, 49]. However, neither thioacetamide nor thiourea can produce a sulfur passivated Ge surface.

To show the advantage of using H_2SO_4/H_2O_2 to clean the Ge surface, the following cleaning treatments were applied to as-received Ge samples before sulfur passivation with $(NH_4)_2S$: cyclic HF/DIW/H_2O_2 rinses, H_2SO_4/H_2O_2 oxidation followed by HF etches and H_2SO_4/H_2O_2 oxidation without following HF etches. The C 1s XPS spectra are shown in

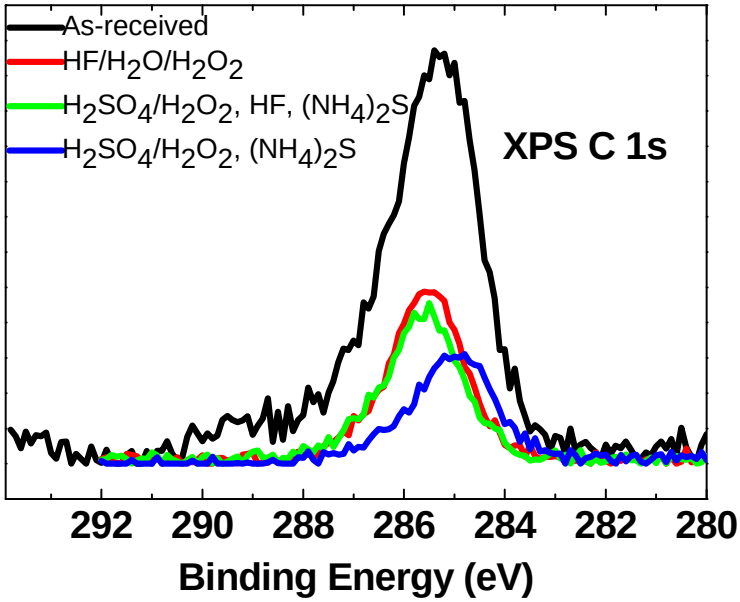

Figure 10 C 1s XPS spectra from sulfur passivated Ge(100) sample with different wet chemistry treatments

Figure 10. In the case of cyclic HF/DIW/H_2O_2 rinses, more carbon is left on the Ge surface and follow-up sulfur passivation using $(NH_4)_2S$ does not help in removing carbon. The sulfur passivated Ge sample pretreated with H_2SO_4/H_2O_2 oxidation has the least amount of carbon. However, if HF etches are applied after H_2SO_4/H_2O_2 oxidation, the carbon amount increases because the removal of the protective chemical oxide makes the cleaned Ge surface more vulnerable to carbon contamination. Therefore, this HF etch should be avoided.

Further analysis of sulfur passivated Ge samples by MEIS yields surface composition and depth profiling of the interface of the sulfur passivation layers. In Figure 11, the modeling of sulfur passivated Ge surface results in an average layer composition of $GeO_{0.2}S_{0.35}$ with the thickness of 18 Å. Sulfur is present with density of 1.0×10^{15} cm^{-2},

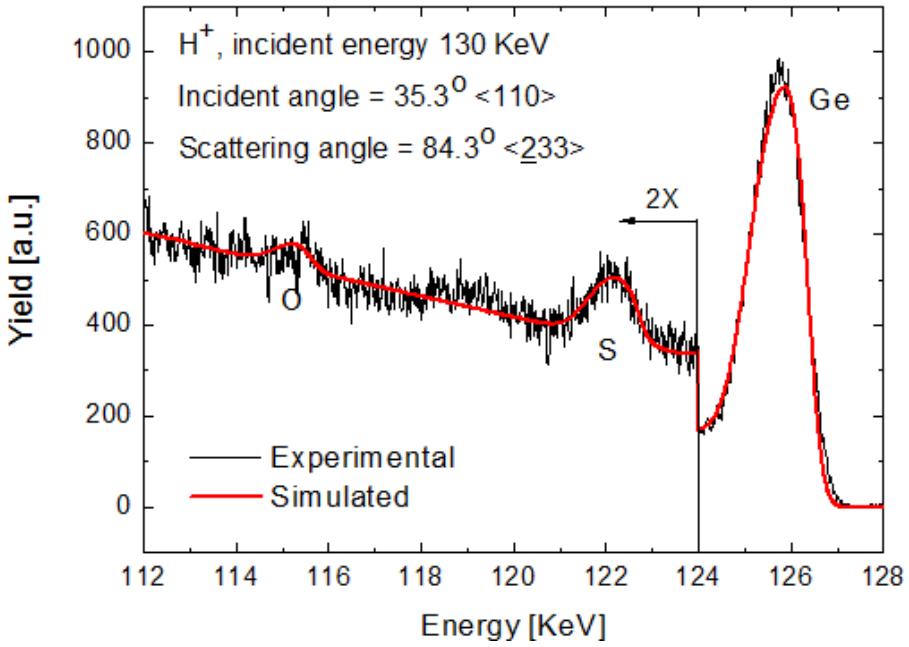

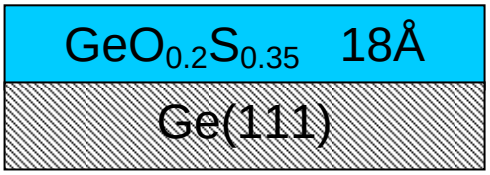

Element	Concentration ×10¹⁵[atoms/cm²]
S	1.0
O	1.5

Figure 11 MEIS spectra of a sulfur passivated Ge(111) surface with interface depth profiling and element density analysis

consistent with literature data [50], and oxygen is present due to air exposure, with smaller than found by others [51]. Almost no carbon signal was detected. With sensitively measured by MEIS, we conclude that sulfur passivation with $(NH_4)_2S$ not only removes the chemical oxide layer but also forms a S/Ge layer which helps passivate the Ge surface. The depth profiling shows a positive result for the sulfur signal on the Ge surface. These two wet chemical treatments together prepare an appropriate Ge substrate for ALD deposition and fabrication of MOSFET devices.

2. Wet chemistry cleaning and sulfur passivation of GaAs

Wet chemistry cleaning for GaAs should be more deeply investigated because the binary surface composition of GaAs produces different oxides of both Ga and As. Figure 12 indicates the Ga 3d and As 3d XPS spectra of as-received GaAs(100). For Ga, the main surface oxide is Ga_2O_3 according to the fitted data [52]. As for As, there are more complicated surface compositions, such as As_2O_5, As_2O_3 and As^0 (As-As) on the surface [53]. The range of different oxides requires different strategies for removing them.

Both acidic (HCl-based [54], H_2SO_4-based [55], HF-based [56]) and basic e.g. (NH_4OH) etching solutions are used for the removal of the surface chemical oxides [57]. Gallium oxides can be easily removed in acidic solutions and arsenic oxides can also be mostly removed. Recent studies have reported that the GaAs surface is covered by gallium chlorides and elemental arsenic after an HCl treatment [58]. On the other hand, arsenic hydroxide and elemental arsenic are found on GaAs surfaces after NH_4OH treatments [58]. The GaAs surface is found to be hydrophobic after HCl and hydrophilic after NH_4OH treatments. In our work, we first use HCl and then NH_4OH for cleaning the GaAs, because the hydrophilic surface is necessary for further ALD processes [59]. After cleaning, hot $(NH_4)_2S$ solution can be used to passivate GaAs surfaces [60]. Similar to Ge, HF etches should be avoided because the deep etching from HF increases surface roughness, very undesireable for the further device fabrication [56].

Figure 13 indicates the Ga 3d and As 3d XPS spectra of a sulfur passivated GaAs surface. From XPS we can see that the oxide layer has been totally removed, there is neither Ga nor As oxide peaks in the fitted XPS curves, and the Ga-S and As-S bond have been generated

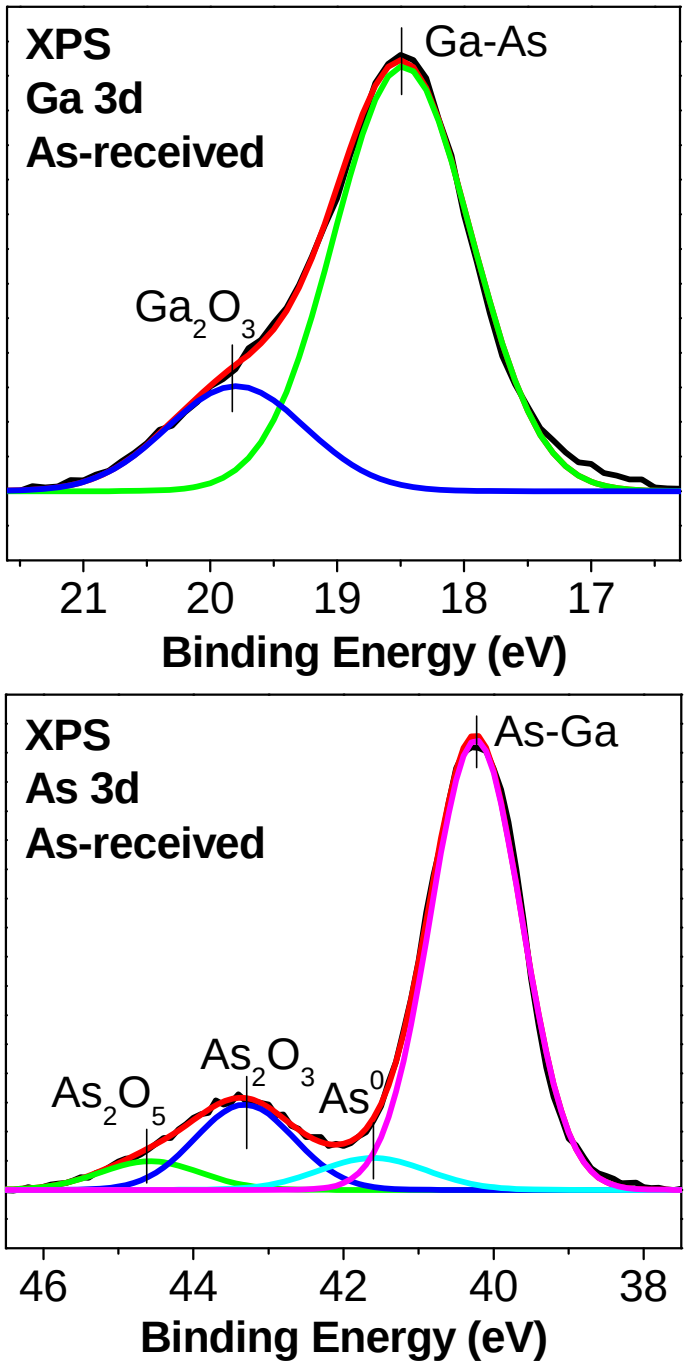

Figure 12 Ga and As 3d XPS spectra of as-received GaAs(100)

on the surface which have smaller binding energy than Ga and As oxide peaks [61]. As expected, the As 2p peak is substaintially more sensitive to the presence of the surface

oxides than the As 3d because of the low kinetic energy of the photoelectrons [53]. We observe the differences in the As 2p spectra after the sulfur passivation. By comparing the as-received As 2p and S-passivated As 2p spectra indicated in Figure 14, we find that

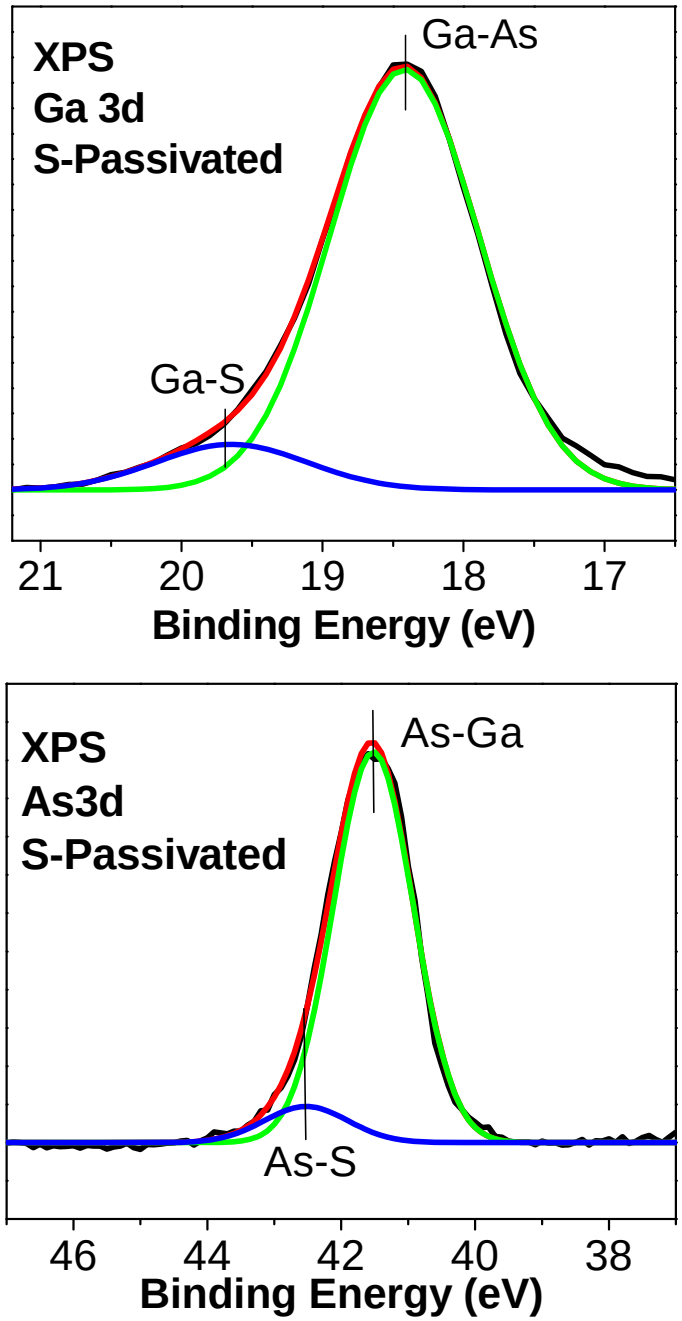

Figure 13 Ga and As 3d XPS spectra of sulfur passivated GaAs(100) after HCl and NH_4OH cleaning

the main As peak of GaAs is much larger after S-passivation, and the oxide peaks decrease, although we can still see some As_2O_3 after the sulfur passivation [62].

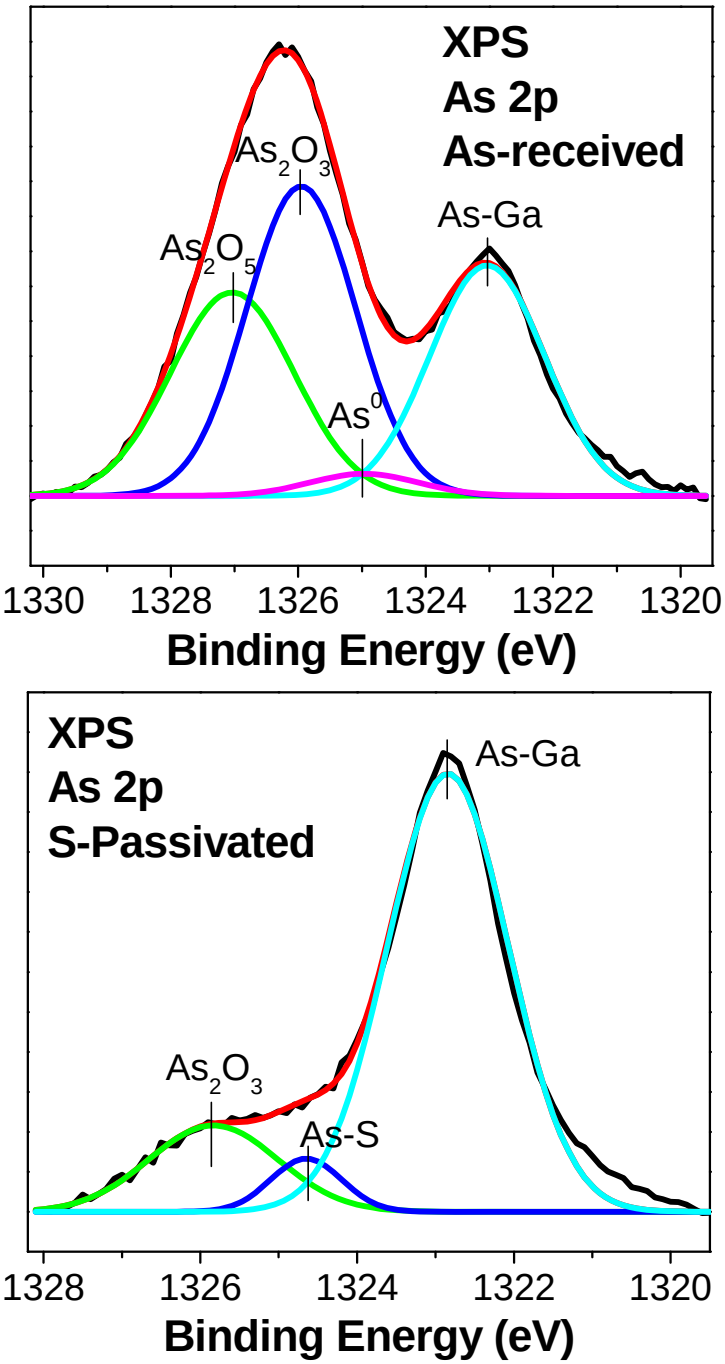

Figure 14 As 2p XPS spectra of as-received (upper) and sulfur passivated (lower) GaAs(100)

3. Atomic Layer Deposition of High-κ dielectric films on Ge and GaAs

In this work, experimental results of ALD growth of Al_2O_3 and HfO_2 on Ge and GaAs substrates are presented; we mainly focus on HfO_2 on Ge growth. We also have examined both Al_2O_3 and HfO_2 film growth on GaAs. We choose TEMAHf as the precursor of HfO_2 and TMA as the precursor of Al_2O_3, using water as the reactant in both cases. The growth temperature of HfO_2 is 170°C and Al_2O_3 is around 70-95°C [63-65]. With the help of RBS, the deposited film thicknesses were determined as well as the growth rates per ALD cycle.

The whole ALD system including the sample is first preheated to 100-110°C to obtain the desorption of water and then pumped down to 10^{-6}-10^{-7} Torr for an hour before the deposition. The flow rate of purging N_2 is set to 100 cc per minute by a mass flow controller. During the deposition, the reactor and all gas lines are heated with heating tape in a hot wall condition at fixed elevated temperature in order to prevent the condensation of chemicals on the chamber walls. Figures 15 and 16 are RBS spectra that result after 35 ALD cycles, yielding 30 Å of HfO_2 on Ge. We also find that 100 Å of Al_2O_3 is deposited after 120 cycles of TMA/H_2O on GaAs. With linear fitting, we can determine the growth rate is 0.86 Å/cycle on Ge and 0.84 Å/cycle on GaAs, which is in agreement with literature data.

After ALD growth of HfO_2 on Ge, we fabricated MOS capacitors with further deposition of a metal electrode. The electric properties indentify that the interface state density is below 10^{11} $eV^{-1}cm^{-2}$. It can be concluded that the semiconductor/high-κ dielectric interface has been improved by our wet chemistry cleaning and sulfur passivation [51]. For the GaAs MOS capacitor with a HfO_2 dielectric layer, the interface is

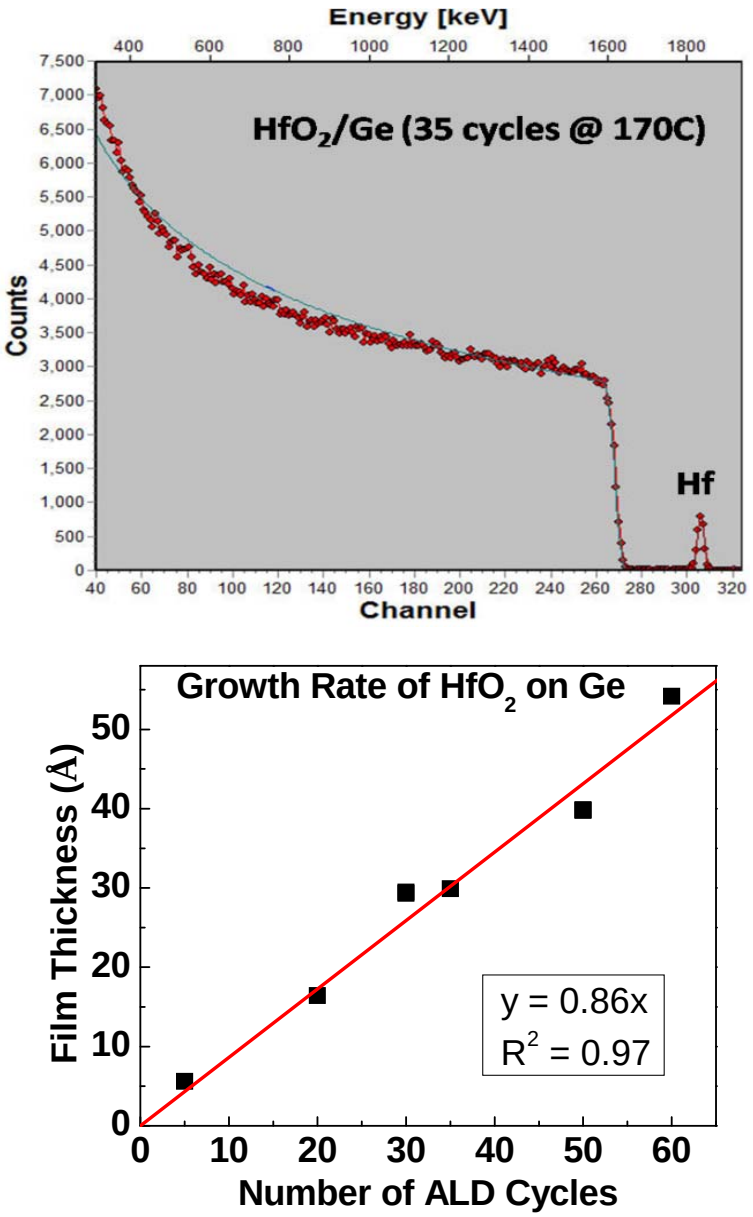

Figure 15 RBS spectra and growth rate of ALD with HfO_2/Ge

still rough through as seen in the TEM images. Figure 17 indicates a cross-sectional TEM image of a gate stack of TaN/HfO_2/GaAs. From the image, we can clearly find roughness at the HfO_2/GaAs interface. It can be concluded that the surface properties of GaAs are more complicated and the wet chemistry cleaning and sulfur passivation of GaAs still do not

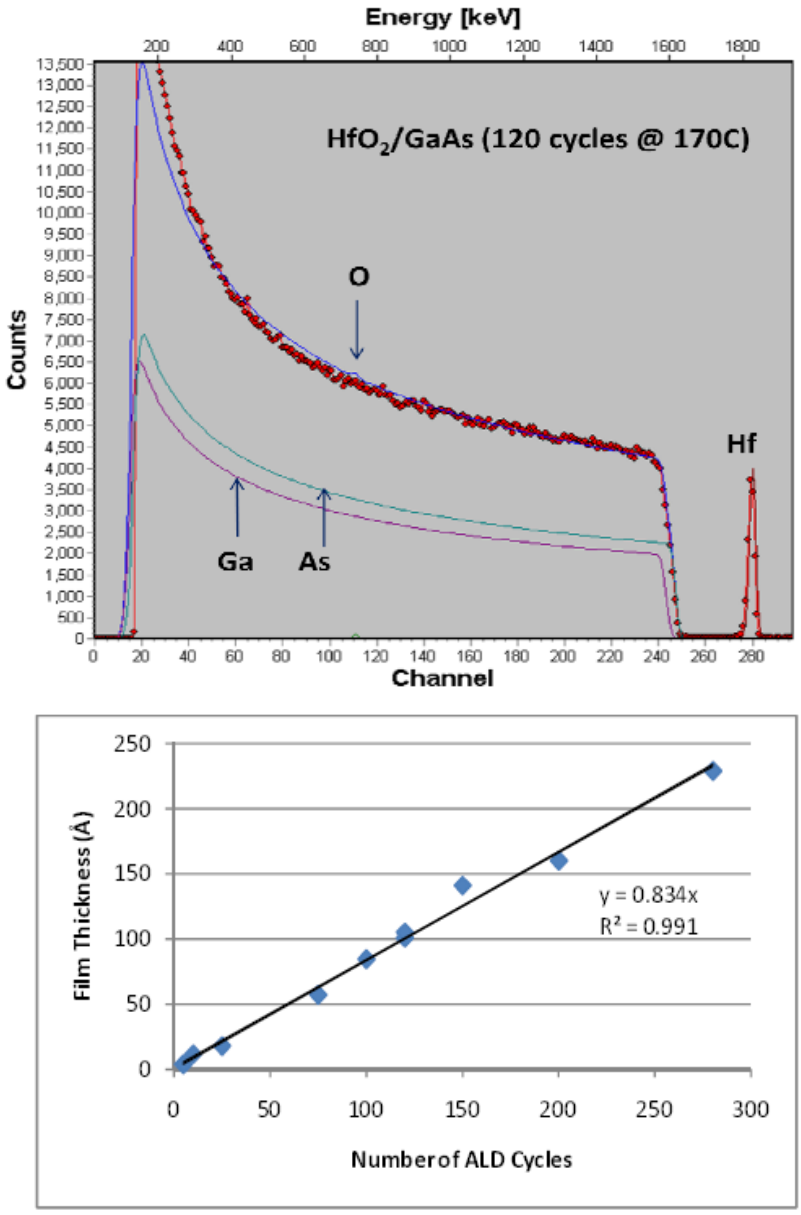

Figure 16 RBS spectra and growth rate of ALD with HfO_2/GaAs

result in reliable interface for ALD growth of HfO_2. It has been reported that there are "self-cleaning" properties during ALD of high-κ dielectrics on GaAs surface as the organometallic precursor can consume the native surface oxide of GaAs, although the exact mechanism is still not clear [62, 66-68]. For further investigation, we will focus on

the surface ALD reactions between the precursor and GaAs, and our *in-situ* ALD-XPS system will be very helpful in these studies.

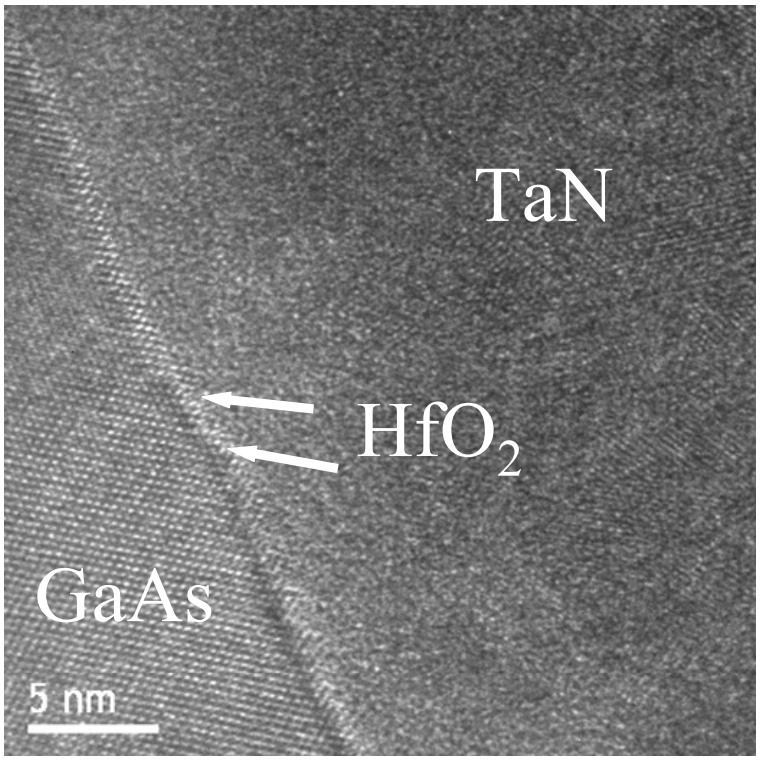

Figure 17 Cross sectional TEM image of the MOS gate stack TaN/HfO_2/GaAs

Chapter 4 Conclusion

Scaling CMOS devices is the key to the development of semiconductor technology. The need for higher performance semiconductors such as Ge and GaAs, which have higher mobility relative to Si, are suggested. Because of the low thermal and chemical stability of native oxides on Ge and GaAs, surface cleaning and preparation are not as straightforward as they are for Si. On the Ge substrate, H_2SO_4/H_2O_2 oxidation not only can greatly reduce the amount of hydrocarbons and carbides, but it also creates a protective oxide to prevent the surface from further contamination in ambient conditions. After the chemical oxide is formed, we also find that HF etches should be avoided in order to reduce the amount of carbon remaining on the Ge surface and to minimize roughening. For GaAs, continuous HCl and NH_4OH can efficiently remove the native oxide of GaAs, and the basic solution forms a hydrophilic surface of GaAs which is preferred for further fabrication.

Surface sulfur passivation is another crucial step in the surface treatment of alternative substrate. With hot aqueous $(NH_4)_2S$ solution, a clean Ge surface without oxides has been demonstrated, and a S/Ge layer has been confirmed with MEIS analysis. Sulfur passivation has efficiently removed the surface oxide and generates a clean passivated surface for further device fabrication. On the GaAs substrate, sulfur passivation also removes and oxide and forms an atomic bond between sulfur and both Ga and As.

Atomic layer deposition proves to be very useful for the growth of ultrathin high-κ dielectric films. In our home-built ALD system, HfO_2 and Al_2O_3 films have been deposited on Ge as well as GaAs substrates. The physical thickness and growth rate have been determined by RBS. Through the combination of our work of wet chemistry cleaning,

surface passivation, and ALD of high-κ dielectric films, we are able to optimize the fabrication of Ge-based MOS capacitors and the electric properties indicate interface improvement with a lower interface state density.

Because of the binary structure and complicated surface properties of GaAs, the interface of high-κ dielectric and semiconductor has not been improved to a level to permit a replacement of Si. For the further investigation, we should optimize the passivation layer of GaAs and control the ALD condition for high-κ film growth. Our integrated system is quite appropriate of *in-situ* experiments for GaAs surface analysis.

Reference

1. Lee, B. H.; Oh, J.; Tseng, H. H.; Jammy, R.; Huff, H. *Mater. Today* **2006**, 9, 32.
2. Chau, R.; Datta, S. Doczy, M.; Doyle, B.; Jin, J.; Kavalieros, J.; Metz, M.; Radosavljevic, M. *IEEE Trans. Nanotechnol.* **2005**, 4, 153.
3. Sze, S. M.; Ng, K. K. *Physics of Semiconductor Devices (Third Edition)*, **2007**, John Wiley & Sons, New York.
4. Loscutoff, P. W.; Bent, S. F. *Annu. Rev. Phys. Chem.* **2006**, 57, 467.
5. Bardeen, J.; Brattain, W. H. *Phys. Rev.* **1948**, 74, 230.
6. Nolte, D. D. *J. Appl. Phys.* **1999**, 85, 6259.
7. Jackson, T. N.; Wong, A. B. *IEEE Electron Device Lett.* **1991**, 12, 605.
8. http://cst-www.nrl.navy.mil/
9. Hasegawa, H.; Akazawa, M. *Appl. Surf. Sci.* **2008**, 254, 8005.
10. Weser, T.; Bogen, A.; Konard, B.; Schnell, R. D.; Schug, C. A.; Steinmann, W. *Phys. Rev. B* **1987**, 35, 8184.
11. Weser, T.; Bogen, A.; Konard, B.; Schnell, R. D.; Schug, C. A.; Moritz, W.; Steinmann, W. *Surf. Sci.* **1988**, 201, 245.
12. Leung, K. T.; Terminello, L. J.; Hussain, Z.; Zhang, X. S.; Hayashi, T.; Shirley, D. A. *Phys. Rev. B* **1988**, 38, 8241.
13. Newstead, K.; Robinson, A. W.; Daddato, S.; Patchett, A.; Prince, N. P.; McGrath, R.; Whittle, R.; Dudzik, E.; McGovern. I. T. *J. Phys.: Condens. Matter* **1992**, 4, 8441.
14. Anderson, G. W.; Hanf, M. C.; Norton, P. R.; Lu, Z. H.; Graham, M. J. *Appl. Phys. Lett.* **1995**, 66, 1123.
15. Lu, Z. H. *Appl. Phys. Lett.* **1996**, 68, 520.
16. Sun, S. Y.; Sun, Y.; Liu, Z.; Lee, D. I.; Peterson, S.; Pianetta, P. *Appl. Phys. Lett.* **2006**, 88, 021903.
17. Choi, K. Buriak, J. M.; *Langmuir*, **2000**, 16, 7737.
18. Bodlaki, D.; Yamamoto, H.; Waldeck, D. H.; Borguet, E. *Surf. Sci.* **2003**, 543, 63.
19. Wong, H. S. P. *IBM J. Res. & Dev.* **2002**, 46, 133.
20. Wilk, G. D.; Wallace, R. M.; Anthony, J. M. *J. Appl. Phys.* **2001**, 89, 5243.
21. Battiston, G. A.; Carta, G.; Cavinato, G.; Gerbasi, R.; Porchia, M.; Rossetto, G. *Chem. Vap. Deposition* **2001**, 7, 69.
22. Ott, A. W.; McCarley, K. C.; Klaus, J. W.; Way, J. D.; George, S. M. *Appl. Surf. Sci.* **1996**, 107, 128.
23. Groner, M. D.; Elam, J. W.; Fabreguette, F. H.; George, S. M. *Thin Solid films* **2002**, 413, 186.
24. Koh, W.; Ku, S. J.; Kim, Y. *Thin Solid Films* **1997**, 304, 222.
25. Lee, P. F.; Dai, J. Y.; Chan, H. L. W.; Choy, C. L. *Ceram. Int.* **2004**, 30, 1267
26. Gusev, E. P.; Cabral, C.; Copel, M.; D'Emic, C.; Gribelyuk, M. *Microelectron. Eng.* **2003**, 69, 145.
27. Han, D. D.; Kang, L. F.; Lin, C. H.; Han, R. Q. *Microelectron. Eng.* **2003**, 66, 643.
28. Renault, O.; Samour, D.; Rouchon, D.; Holliger, P.; Papon, A. M.; Blin, D.; Marthon, S. *Thin Solid Films* **2003**, 428, 190.
29. Ferrari, S.; Dekadjevi, D. T.; Spiga, S.; Tallarida, G.; Wiemer, C.; Fanciulli, M. *J. Non-Cryst. Solids* **2002**, 303, 29.

30. Lin, Y. S.; Puthenkovilakam, R.; Chang, J. P.; Bouldin, C.; Levin, I.; Nguyen, N. V.; Ehrstein, J.; Sun, Y. Pianetta, P.; Conard, T.; Vandervorst, W.; Venturo, V.; Selbrede, S. *J. Appl. Phys.* **2003**, 93, 5945.
31. Wu, X.; Landheer, D.; Graham, M. J.; Chen, H. W.; Huang, T. Y.; Chao, T. S. *J. Cryst. Growth* **2003**, 250, 479.
32. Boughaba, S.; Islam, M.; McCaffrey, J. P.; Sproule, G. I.; Graham, M. J. *Thin Solid Films* **2000**, 371, 119.
33. Boughaba, S.; Sproule, G. I.; McCaffrey, J. P.; Islam, M.; Graham, M. J. *Thin Solid Films* **2000**, 358, 104.
34. Mao, A. Y.; Son, K. A.; Hess, D. A.; Brown, L. A.; White, J. M.; Kwong, D. L.; Roberts, D. A.; Vrtis, R. N. *Thin Solid Films* **1999**, 349, 230.
35. van Dover, R. B.; Lang, D. V.; Green, M. L.; Manchanda, L. *J. Vac. Sci. Technol. A* **2001**, 19, 2779.
36. Zhao, C.; Richard, O.; Young, E.; Bender, H.; Roebben, G.; Haukka, S.; De Gendt, S.; Houssa, M.; Carter, R.; Tsai, W.; Van ber Biest, O.; Heyns, M. *J. Non-Cryst. Solids* **2002**, 303, 144.
37. Suntola, T.; Antson, J.; U. S. Patent 4,058,430, **1977**.
38. Laskelä, M.; Ritala, M. *Angew. Chem. Int. Ed.* **2003**, 42, 5548.
39. Kim, H.; Lee, H. B. R.; Maeng, W. J. *Thin Solid Films* **2009**, 517, 2563.
40. Knez, M.; Nielsch, K.; Niinistö, L. *Adv. Mater.* **2007**, 19, 3425.
41. Prabhakarana, K.; Ogino, T. *Surf. Sci.* **1995**, 325, 263.
42. Schmeisser, D.; Schnell, R. D.; Bogen, A.; Himpsel, F. J.; Rieger, D.; Landgren, G.; Morar, J. F. *Surf. Sci.* **1986**, 172, 455.
43. Rivillon, S.; Chabal, Y. J.; Amy, F.; Kahn, A. *Appl. Phys. Lett.* **2005**, 87, 253101.
44. Deegan, T.; Hughes, G. *Appl. Surf. Sci.* **1998**, 123, 66.
45. Okumura, H.; Akane, T.; Matsumoto, S. *Appl. Surf. Sci.* **1998**, 125, 125.
46. Zhang, X. J.; Xue, G.; Agarwal, A.; Tsu, R. Hasan, M. A.; Greene, J. E.; Rockett, A. *J. Vac. Sci. Technol. A* **1993**, 11, 2553.
47. Maeda, T.; Takagi, S.; Ohnishi, T. Lippmaa, M. *Mat. Sci. Semicon. Proc.* **2006**, 9, 706.
48. Petrovykh, D. Y.; Long, J. P.; Whitman, L. J. *Appl. Phys. Lett.* **2005**, 86, 242105.
49. Petrovykh, D. Y.; Sullivan, J. M.; Whitman, L. J. *Surf. Interface Anal.* **2005**, 37, 989.
50. Lyman, P. F.; Sakata, O.; Marasco, D. L.; Lee, T. L.; Breneman, K. D.; Keane, D. T.; Bedzyk, M. J. *Surf. Sci.* **2000**, 462, L594.
51. Frank, M. M.; Koester, S. J.; Copel, M.; Ott, J. A.; Paruchuri, V. K.; Shang, H.; Loesing, R. *Appl. Phys. Lett.* **2006**, 89, 112905.
52. Shahrjerdi, D; Garcia-Gutierrez, D. I.; Akyol, T.; Bank, S. R.; Tutuc, E.; Lee, J. C.; Banerjee, S. K. *Appl. Phys. Lett.* **2007**, 91, 193503.
53. Hackley, J. C.; Demaree, J. D.; Gougousi, T. *Appl. Phys. Lett.* **2008**, 92, 162902.
54. Tereshchenko, O. E.; Chikichev, S. I.; Terekhov, A. S. *J. Vac. Sci. Technol. A* **1999**, 17, 2655.
55. Liu, Z.; Sun, Y.; Machuca, F.; Pianetta, P.; Spicer, W. E.; Pease, R. F. W. *J. Vac. Sci. Technol. A* **2003**, 21, 212.
56. Adachi, S; Kikuchi, D. *J. Electrochem. Soc.* **2000**, 147, 4618.
57. Lebedev, M. V.; Ensling, D.; Hunger, R.; Mayer, T.; Jaegermann, W. *Appl. Surf. Sci.* **2004**, 229, 226.

58. Lebedev, M. V.; Mankel, E.; Mayer, T.; Jaegermann, W. *J. Phys. Chem. C* **2008**, 112, 18510.
59. Xuan, Y.; Lin, H. C.; Ye, P. D. *IEEE Trans. Electron Devices* **2007**, 54, 1811.
60. Arabasz, S.; Bergignat, E.; Hollinger, G.; Szuber, J. *Appl. Surf. Sci.* **2006**, 252, 7659.
61. Aguirre-Tostado, F. S.; Milojevic, M.; Choi, K. J.; Kim, H. C.; Hinkle, C. L.; Vogel, E. M.; Kim, J.; Yang, T.; Xuan, Y.; Ye, P. D.; Wallace, R. M. *Appl. Phys. Lett.* **2008**, 93, 061907.
62. Hinkle, C. L.; Sonnet, A. M.; Vogel, E. M.; McDonnell, S.; Hughes, G. J.; Milojevic, M.; Lee, B.; Aguirre-Tostado, F. S.; Choi, K. J.; Kim, H. C.; Kim, J.; Wallace, R. M. *Appl. Phys. Lett.* **2008**, 92, 071901.
63. Hausmann, D. M.; Kim, E.; Becker, J.; Gordon, R. G. *Chem. Mater.* **2002**, 14, 4350.
64. Kukli, K.; Ritala, M.; Sajavaara, T.; Keinonen, J.; Leskelä, M. *Chem. Vap. Deposition* **2002**, 8, 199.
65. Yun, S. J.; Lee, K. H.; Skarp, J.; Kim, H. R.; Nam, K. S. *J. Vac. Sci. Technol. A* **1997**, 15, 2993.
66. Frank, M. M.; Wilk, G. D.; Starodub, D.; Gustafsson, T.; Garfunkel, E.; Chabal, Y. J.; Grazul, J.; Muller, D. A. *Appl. Phys. Lett.* **2005**, 86, 152904.
67. Chang, C. H.; Chiou, Y. K.; Chang, Y. C.; Lee, K. Y.; Lin, T. D.; Wu, T. B.; Hong, M.; Kwo, J. *Appl. Phys. Lett.* **2006**, 89, 242911.
68. Shahrjerdi, D.; Nuntawong, N.; Balakrishnan, G.; Garcia-Gutierrez, D. I.; Khoshakhlagh, A.; Tutuc, E.; Huffaker, D.; Lee, J. C.; Banerjee, S. K. *J. Vac. Sci. Technol. B* **2008**, 26, 1182.